Understanding How in Situ Generated Hydrogen Controls the Morphology of Platinum Nanoparticles

Neus Aguilera-Porta, Monica Calatayud, Caroline Salzemann, Christophe Petit

THE JOURNAL OF PHYSICAL CHEMISTRY C

Article

pubs.acs.org/JPCC

Understanding How in Situ Generated Hydrogen Controls the Morphology of Platinum Nanoparticles

Neus Aguilera-Porta,[†,‡,§,∥] Monica Calatayud,*[,†,‡,⊥] Caroline Salzemann,[§,∥] and Christophe Petit*[,§,∥]

[†]Sorbonne Universités, UPMC Univ Paris 06, UMR 7616, Laboratoire de Chimie Théorique, F-75005 Paris, France

[‡]CNRS, UMR 7616, Laboratoire de Chimie Théorique, F-75005 Paris, France

[§]Sorbonne Universités, UPMC Univ Paris 06, UMR 8233, Laboratoire MONARIS, F-75005 Paris, France

[∥]CNRS, UMR 8233, Laboratoire MONARIS, F-75005 Paris, France

[⊥]Institut Universitaire de France, F-75252 Paris, France

Supporting Information

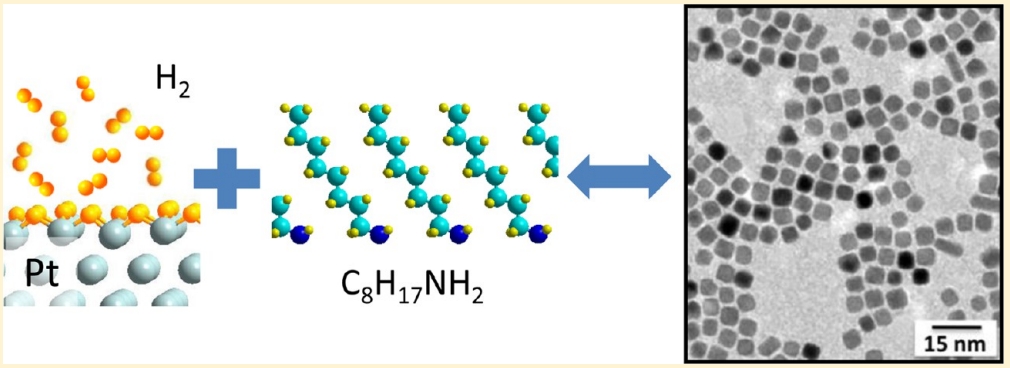

ABSTRACT: Small adsorbed molecules play a key role in the morphology of inorganic nanoparticles. The presence of in situ generated hydrogen during the synthesis of platinum nanoparticles is found to drive the growth of cubic nanocrystals, but little is known about the processes occurring at the molecular level. In this paper, we use standard ab initio calculations to show that hydrogen preferentially adsorbs on (100) Pt facets compared to (111) stabilizing the cubic morphology. Moreover, we provide experimental and theoretical evidence that moderate partial pressure of hydrogen is needed to obtain nanocubes. In the absence of hydrogen, or for low partial pressures, small nanoparticles with undefined shape are formed; however, longer exposure to hydrogen pressure around 1 atm leads to the formation of cubes. Finally, this theoretical result allows presenting an experimental protocol to be used to obtain platinum nanocubes with different degree of truncation.

INTRODUCTION

Many physical and chemical properties depend on the shape of the particles forming the material,[1] hence the challenge of controlling the crystal morphology in a wide range of scientific and technological applications. The chemical route is largely used to control the shape of inorganic nanocrystals, although there is still no theoretical drawback of the main forces driving it. Despite many studies found in the literature, the theoretical and computer simulation of nanoparticles' synthesis and growth are still in the initial stage of development, and most of these works do not take into account the complexity of the chemical synthesis. It is still paramount to explain the mechanisms at the origin of the uniformity of shape. Indeed, the field is still wide open to future research aiming at identifying the conditions to control the nanomorphology.

In the chemical synthesis of the nanocrystals, the chemical bath possesses a complex composition containing various reactants, solvents, surfactants, (counter)ions, and impurities. Moreover, during the reaction, byproducts can be formed, which could play a role in the nuclei formation and the following nanoparticles' growth.[2] For instance, the role of dissolved gas H_2 on the shape control of platinum nanocrystals has recently been demonstrated experimentally.[3] Some authors also report the role of halide, ligands, or adsorbed CO on the nanomorphology.[4−6] Besides, the role of the initial shape of the nanocrystals and the growth kinetics have been emphasized.[7,8] Beyond the experimental recipe, a theoretical approach is needed to rationalize and predict the stability of the nano-objects. In the present paper, the goal is to emphasize the role of a byproduct generated during the chemical synthesis in the final nanoparticle morphology. We focus here on the specific case of platinum. We use ab initio calculations to explain how the presence of in situ generated H_2 drives the formation of cubic nanoparticles. We also explain the impact of the experimental conditions, namely, the partial

Received: March 3, 2014
Revised: April 7, 2014

   dx.doi.org/10.1021/jp502174b | J. Phys. Chem. C XXXX, XXX, XXX−XXX

pressure of hydrogen and the order of addition of reactants in the chemical bath: the nanocubes are obtained *only* following a particular experimental protocol (i) when the surfactant agent is added after the reducing hydrogen and (ii) in the presence of moderate hydrogen partial pressure. If one of these conditions is not satisfied, nanowires made of aggregated nanospheres are obtained. Interestingly, it is possible to obtain nanocubes with a selected degree of truncation by controlling the time of extraction of the nanoparticles. Beyond the specific case of the platinum, we believe that this approach based on theory and experiment allows gaining further understanding of the shape control of metallic nanocrystals obtained by the chemical route, and furthermore, this approach may be a powerful tool of general application in the field of nanocrystal synthesis.

The morphology of a given crystal is governed by the stability of the interface between the solid phase and the media. The crystal grows following the most stable surface termination. Therefore, the interaction of the substrate−adsorbate system is crucial to understand mechanisms of stabilization for a given morphology. A way of predicting the morphology of a crystal is thus to calculate the energies of the different surfaces, the predominant surface will be that of lower energy. Different approaches based on the Wulff construction exist to predict the crystalline shape (for instance, see ref). Pt crystallizes in the face-centered cubic system which has two major surface terminations: (111) and (100). Predominance of the former will lead to octahedral particles, whereas the latter leads to cubic shapes. In this paper, we present an approach to calculate the surface energy of (111) and (100) terminations in different conditions (bare, hydrogenated, and capped by a surfactant molecule) by standard periodic density functional theory (DFT) calculations. The factors stabilizing each termination will be analyzed, and the results will be compared with the particles synthesized under different conditions. A protocol to obtain cubic particles with a degree of truncation will be proposed.

■ EXPERIMENTAL SECTION

Pt nanocrystals are synthesized by the phase transfer synthesis method presented by Brust et al.[10] Typically, it consists of metal ion transfer from an aqueous phase to an organic phase using an extractant molecule. The nanocrystals are obtained by chemical reduction. This method separates the nucleation media (the water/toluene interface) from the growth media (toluene) yielding to a well-dispersed NP organic solvent.[11]

The metallic salt solution is prepared as follows: aqueous solutions of 3.3×10^{-2} M $PtCl_4$ were prepared by dissolving the metallic salt in acid media (1/3 HCl 37% to 2/3 H_2O) to form the complexes H_2PtCl_6. After stirring during 1 h, this aqueous solution is then mixed with 1.9×10^{-2} M tridecylammonium bromide (TDAB) dispersed in 80 mL of toluene. To ensure maximum transfer of metal ions from the water phase to the organic phase, the transferring agent (TDAB) was present in large excess (corresponding to TDAB/$PtCl_4$ = 3/1) and the extraction occurs in four steps; TDAB/toluene solution (20 mL) is added to the acidic solution containing the metallic salt, the two-phases mixture was vigorously stirred until all the metallic complexes were transferred into the organic phase (30 min). The organic phase is collected and 20 mL of TDAB/toluene is added again. Finally, the four fractions are combined. The colorless water phase is then discarded.

Chemical Reduction of the Metallic Salt. *Procedure I: Reduction in the Presence of the Capping Agent.* Initially, 6.10^{-3} mol of octylamine ($C_8H_{17}NH_2$) capping agent (CA) is added under stirring to 10 mL of the obtained organic solution containing the metallic complexes. A freshly prepared aqueous solution of $NaBH_4$ (10 mL, 1 mol·L^{-1}) is dropwise added under stirring, yielding to an emulsion. This induces the reduction of the metallic salt at the interface of the organic and aqueous phases. Both the reducing agent and the capping agent are added in large stoichiometric excess relative to the platinum ($NaBH_4$/Pt^{4+} =160:1 and CA/Pt = 96:1). The emulsion turns relatively fast from orange to dark brown. The reaction takes place for one night after what the stirring has removed, and the organic phase, containing the metal nanoparticles, is collected and evaporated using a Rotavapor. The black paste obtained is then washed with 40 mL of ethanol. Then, the turbid solution is centrifuged, and the supernatant is discarded. This operation is repeated twice. After the last centrifugation, the precipitate is redispersed in 4 mL of toluene. The final solution contains the coated C_8NH_2 nanoparticles in toluene.

Procedure II: Reduction Followed by the Addition of Capping Agent. In this case, the freshly prepared aqueous solution of $NaBH_4$ (10 mL, 1 mol·L^{-1}) is dropwise added under stirring to 10 mL of the organic solution containing the metallic complexes. The reduction occurs in the emulsion phase, at the interface of the organic and aqueous phases, which results in a color change from orange to dark brown. After 60 min (ripening time τ_{rip}), 6. 10^{-3} mol of octylamine is then added. The chemical bath is kept under stirring for one night, and then the nanocrystals are extracted following the procedure described above. The final solution contains the coated C_8NH_2 nanoparticles in toluene.

Environmental Effect. The synthesis of Pt NCs has been performed both in the presence and in the absence of hydrogen atmosphere under glovebox with outgassed solutions.

Hydrogen is naturally produced by the chemical reduction. To perform the reaction under saturated H_2 atmosphere, a closed screw cap with three ports is used, and both the reducing and the capping agent are injected through a silicone septum. In order to see the influence of hydrogen atmosphere on the nanoparticles, we performed the same syntheses with open screw cap and by bubbling N_2 into the chemical bath, during and after the reduction, to drive out the hydrogen formed.

In order to see the influence of the overpressure of H_2 (see Discussion and Figure 7), the capping agent is added at a specific time, not using the silicon septum but opening the vessels. This yields to a drastic decrease of the overpressure.

The TEM micrographs are obtained on a JEOL 1011 apparatus, HRTEM are obtained on a JEOL 2010.

Computational Methods and Models. The VASP code[12,13] is used with the revised Perdew−Becke−Erzernhof functional rPBE. The core electrons are represented by pseudopotentials generated by the projector augmented wave (PAW) method.[14,15] The valence electrons (Pt: 10; N: 5; C: 4; H: 1) are described by plane-wave basis sets with a cutoff of 400 eV. A $5 \times 5 \times 1$ k-points scheme is used in the Brillouin zone. The following unit cells were used (100): c2 × 2, 5.635 × 5.635 × 35 Å^3; (111): 2 × 2, 5.628 × 5.628 × 35 Å^3, including a vacuum of ∼20 Å to prevent interaction between successive slabs. The thickness of the slabs is five layers, each layer containing four Pt atoms, see Figure 2. The unit cells are chosen to have similar surface area and equal composition of the slab (20 atoms each) so that the total energy can be easily compared. The three uppermost Pt layers are relaxed during the optimization procedures together with the adsorbates, and the two bottom layers are frozen to the ideal bulk positions. The ionic

dx.doi.org/10.1021/jp502174b | J. Phys. Chem. C XXXX, XXX, XXX−XXX

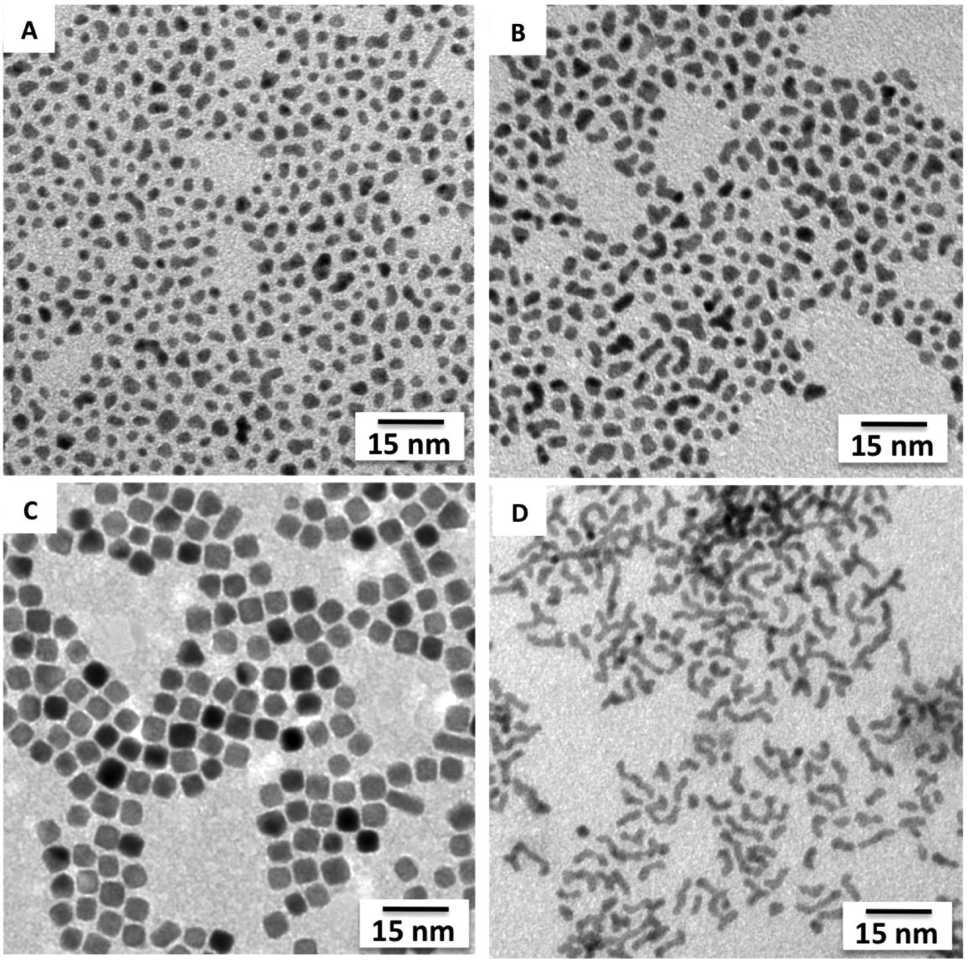

Figure 1. TEM images of platinum nanocrystals coated by octylamine and redispersed in toluene. A drop of solution is deposited on a TEM grid. (A) and (B) Synthesis made following the procedure I (i.e., capping agent added *before* the reducing agent) in the presence (A) or in the absence (B) of hydrogen. (C) and (D) Synthesis made following the procedure II (i.e., capping agent added *after* the reducing agent) in the presence (C) or in the absence (D) of hydrogen.

convergence is achieved for total energy until the difference was below 1 meV; the conjugate gradient method was employed. Periodic DFT has been successfully used in the past to describe adsorption systems and gold self-assembled monolayers.[16,17] Dispersion forces have been included as implemented in the Grimme-D2 approach,[18] for the adsorbates and the first slab layer as in ref 19. The parameters used are given as Supporting Information.

We consider the reaction of adsorption between the slab and N molecules of type M (hydrogen or octylamine)

$$\text{slab} + \text{N}\cdot\text{M} = [\text{slab} - \text{NM}] \quad (1)$$

The stability of a given slab may be calculated as the reaction energy associated with eq 1

$$\Delta G_r = G_{[\text{slab}-\text{NM}]} - G_{\text{slab}} - N\mu_M \quad (2)$$

where G_i are the Gibbs free energies of the covered and bare slabs, μ_M is the chemical potential of the adsorbate M. Because we are interested in the *relative* stability between bare and covered slabs, volume and entropy changes can be neglected assuming that they are equal for the two slabs. The Gibbs energy can then be replaced by the internal energy of each slab as directly obtained from the total-energy calculations. We have chosen the (111) termination as reference for the bare slab, and the $1/2H_2$ (or octylamine) gas-phase energy as reference for the covered slabs.

RESULTS AND DISCUSSION

Platinum nanocrystals (NCs) are obtained from chemical reduction by an aqueous solution of sodium borohydrate ($NaBH_4$, reducing agent) of a metallic salt solubilized in toluene.[3,20] To stabilize the nanoparticles, octylamine molecules ($C_8H_{17}NH_2$, surfactant agent denoted as C_8NH_2) are used as passivating agent that can be added either before (procedure I) or 1 h after (procedure II) the addition of the reducing agent.[3] In such a synthesis, the chemical reduction takes place at the water/oil interface under stirring which allows separating the nucleation and the growth steps, yielding to calibrated nanocrystals with low size dispersion.[11] In this synthesis, the passivating agent is weakly bound to the metallic surface (physisorbed) and the reaction produces hydrogen spontaneously. Thus, a competition occurs between C_8NH_2 and H_2 in interaction with the metallic surface, allowing the size and shape control of the nanoparticles.[3] In order to investigate such competition, the order of addition considered in procedures I and II has been studied, whereas the role of the in situ generated hydrogen has been evidenced by carrying out synthesis in the presence and in the absence of hydrogen. The presence of a moderated pressure of H_2 is achieved by working with closed vessels, whereas the absence of H_2 is studied by

dx.doi.org/10.1021/jp502174b | J. Phys. Chem. C XXXX, XXX, XXX−XXX

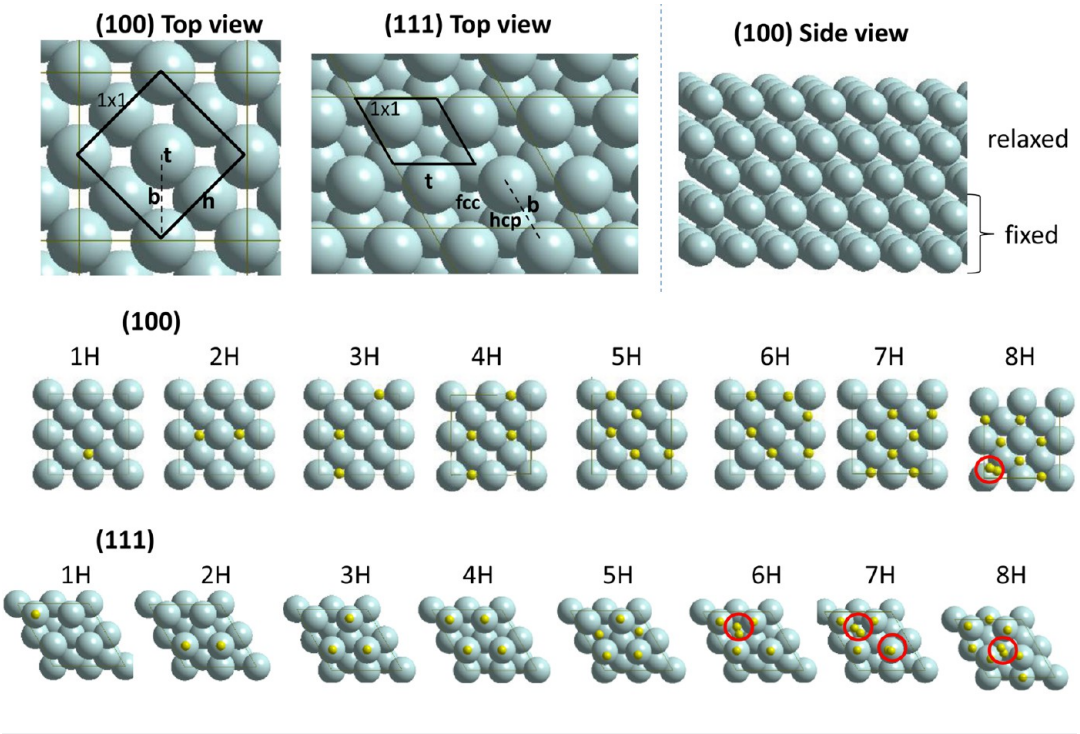

Figure 2. Most stable structures for bare slabs (top) and hydrogen-covered slabs (bottom). The 1 × 1 unit cells are displayed: b, bridging; t, top; h, hollow. Red circles indicate H_2 molecules.

bubbling N_2 during the reaction that drives out the hydrogen formed.

Figure 1 shows the coated C_8NH_2−Pt NCs obtained after extraction and redispersion in toluene. To minimize the external factors, they are synthesized under glovebox with outgassed solutions, as O_2 perturbs the formation of platinum nanocrystals.[20] The Pt nanoparticles obtained from procedure I in the presence (Figure 1A) or in the absence (Figure 1B) of hydrogen are characterized by a mean diameter of around 2.4 nm and a size dispersion of 21%. No clear size and shape effect is observed between both samples. In contrast, the synthesis performed by procedure II leads to drastic changes of both size and shape of the nanoparticles. Indeed, 4.5 nm Pt nanocubes having 13% size dispersion are obtained in the presence of hydrogen (Figure 1C), and platinum nanowires characterized by a cross sectional diameter of 2.0 nm have been obtained without hydrogen (Figure 1D). Thus, the synthesis conditions (i.e., the presence or absence of H_2 in the solution) together with the order of addition of the capping agent, strongly influence the platinum nanomorphology. In the following, we will investigate theoretically the respective role of these different elements on the shape control.

Periodic DFT calculations have been carried out to compute the stability of the terminations of (111) and (100) slabs. The bare (111)-terminated slabs are found to be more stable than the (100)-terminated ones in agreement with the literature,[21] and thus in vacuum conditions, octahedral particles are expected to be formed. For the covered slabs, we have considered the interaction of hydrogen and of the surfactant octylamine. For the hydrogen case, we consider the adsorption of 1 to 8 hydrogen atoms on the slabs. Experiments and calculations find that there exist low barrier pathways for the dissociation of dihydrogen on Pt,[22−24] so we consider only atomic hydrogen. Figure 2 displays the optimized systems for all the compositions considered. It is shown that the (100) slab shows a high affinity for adsorbing atomic H: Up to 7H, the slab is covered by H. For higher coverage, the adsorbed atoms recombine to form H_2 that leaves the surface, whereas the hydrogenated (111) termination is stable only up to 5H. Beyond this value, H_2 is formed. The higher affinity of hydrogen for (100) with respect to (111) is also observed in the calculated adsorption energies shown in Table 1, Figure S1, where the adsorption per H atom is always more exothermic for (100) than for (111). The calculated adsorption energy values are in agreement with those reported in the

Table 1. Calculated Adsorption Energy for the Hydrogenated and Octylamine Covered Slabs[a]

	E_{ads} (111)	E_{ads} (100)	E_{ads} (100)/(111)	predicted shape
0H	−112.35[c]	−110.49[c]	0.98	truncated octahedron
1H	−0.41	−0.53	1.29	cube
2H	−0.38	−0.52	1.36	cube
3H	−0.29	−0.52	1.77	cube
4H	−0.35	−0.51	1.47	cube
5H	−0.21	−0.46	2.17	cube
6H	−0.23[b]	−0.41	1.76	cube
7H	−0.17[b]	−0.37	2.20	cube
8H	−0.16[b]	−0.31[b]	1.95	cube
C_8NH_2	−1.16	−1.19	1.03	truncated octahedron

[a]Values are in eV, calculated as $E_{ads} = (E_{NM} - E_{slab} - NE_M)/N$, where M is $1/2H_2$ or C_8NH_2 molecule calculated in the gas phase, and E_{slab} refers to the reference energy for each slab. $E_{ads}(100)/(111)$ measures the relative stability of the two terminations: values >1 indicate predominance of cubic, values <1 indicate predominance of octahedral particles, and values close to 1 indicate truncated cubes. [b]Molecular H_2 is formed. [c]Total energy.

dx.doi.org/10.1021/jp502174b | J. Phys. Chem. C XXXX, XXX, XXX−XXX

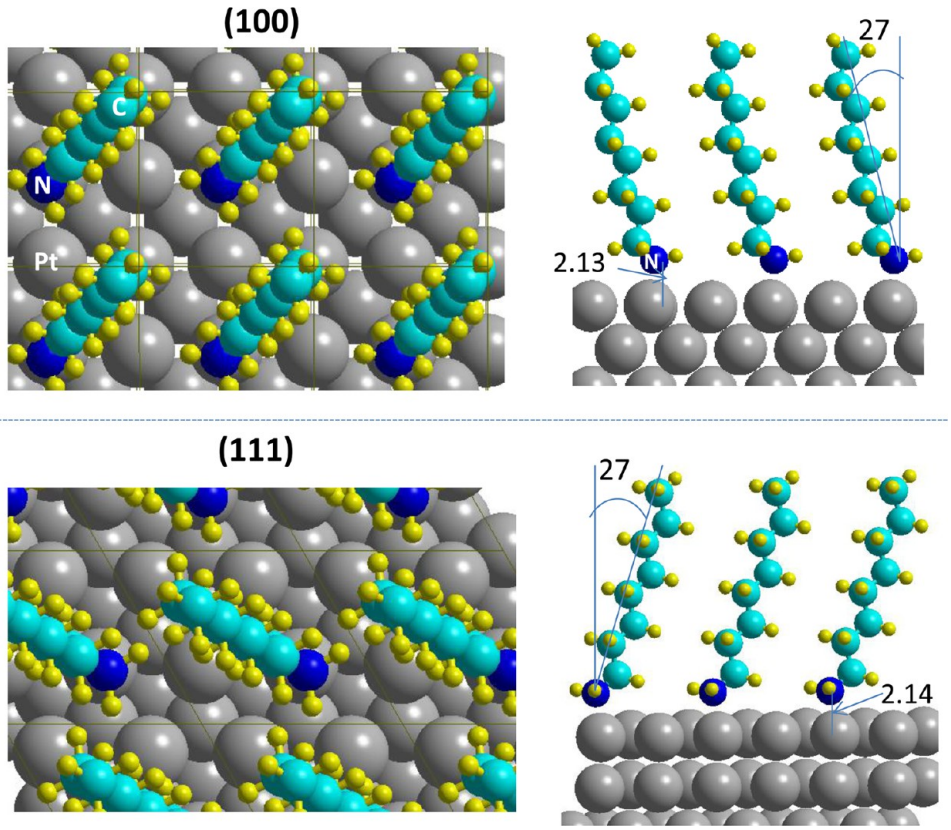

Figure 3. Top and side views of the C_8NH_2 molecule adsorbed on the model slabs. Angles in degrees, N−Pt distance in Å.

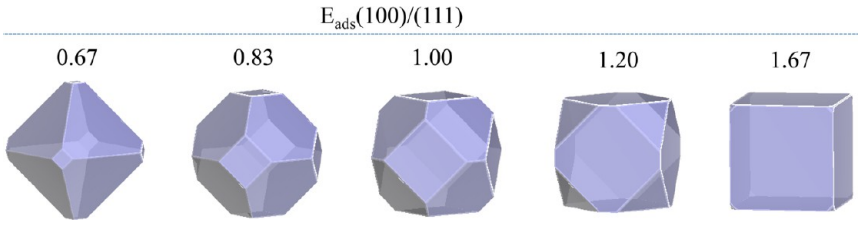

Figure 4. Morphology of Pt particles predicted from ab initio calculations. The adsorption energy of a reactant on each slab serves to compute the exposed area of each termination. The ratio between the adsorption energies $E_{ads}(100)/(111)$ is a measure of the shape: the particle is cubic (values higher than 1.6), octahedral (values lower than 0.7), or truncated (intermediate values).

literature for similar computational approaches.[25,26] As regards the adsorption site, hydrogen is found to adsorb on bridging sites for the (100) slab and a mixture between bridge, top, and hollow sites for the (111) slab, in agreement with previous calculations.[25]

The adsorption of octylamine is also computed for comparison. The molecule is found to adsorb on quasi-top sites in both surfaces, tilted 27° from the vertical of the slab (see Figure 3). The calculated adsorption energies for the two slabs shown in Table 1 are very similar: −1.16 eV (111) and −1.19 eV (100). These results indicate that C_8NH_2 adsorbs more strongly than hydrogen on the Pt surfaces. Contrary to the hydrogen adsorption, the octylamine molecule has no clear preference for a given termination. In the following, we will focus on the hydrogen adsorption, because experiments and theoretical results highlight its crucial role in the synthesis.

The shape of platinum nanoparticles can be qualitatively predicted from the ab initio calculated adsorption energies. The most exposed planes will be those growing more slowly (i.e., the most stable). Taking the *ratio* of the adsorption energies on each of the slabs, $E_{ads}(100)/(111)$ can be used as a measure of the relative stability of the (100) slab with respect to (111). A sketch of the so-calculated shapes is displayed in Figure 4. For $E_{ads}(100)/(111)$ values close to 1, the two terminations are almost equivalent in energy and will expose the same area leading to truncated octahedral morphology. As the $E_{ads}(100)/(111)$ value becomes higher than 1, the (100) termination becomes more stabilized, and the particle tends to form a cubic shape; the opposite behavior leads to octahedral-shaped particles.

In order to compare the relative stability of the slabs under the same external conditions we have carried out a thermodynamic analysis. The stability of a given slab in the presence of an external reactant M may be calculated as the reaction energy associated with eq 1a

$$\text{slab} + \text{NM} = [\text{slab} - \text{NM}] \quad (1a)$$

$$\Delta G_r = G_{[\text{slab}-\text{NM}]} - G_{\text{slab}} - N\mu_M \quad (2a)$$

where G_i are the Gibbs free energies of the covered and bare slabs, μ_M is the chemical potential of the reactant M, N being its

dx.doi.org/10.1021/jp502174b | J. Phys. Chem. C XXXX, XXX, XXX−XXX

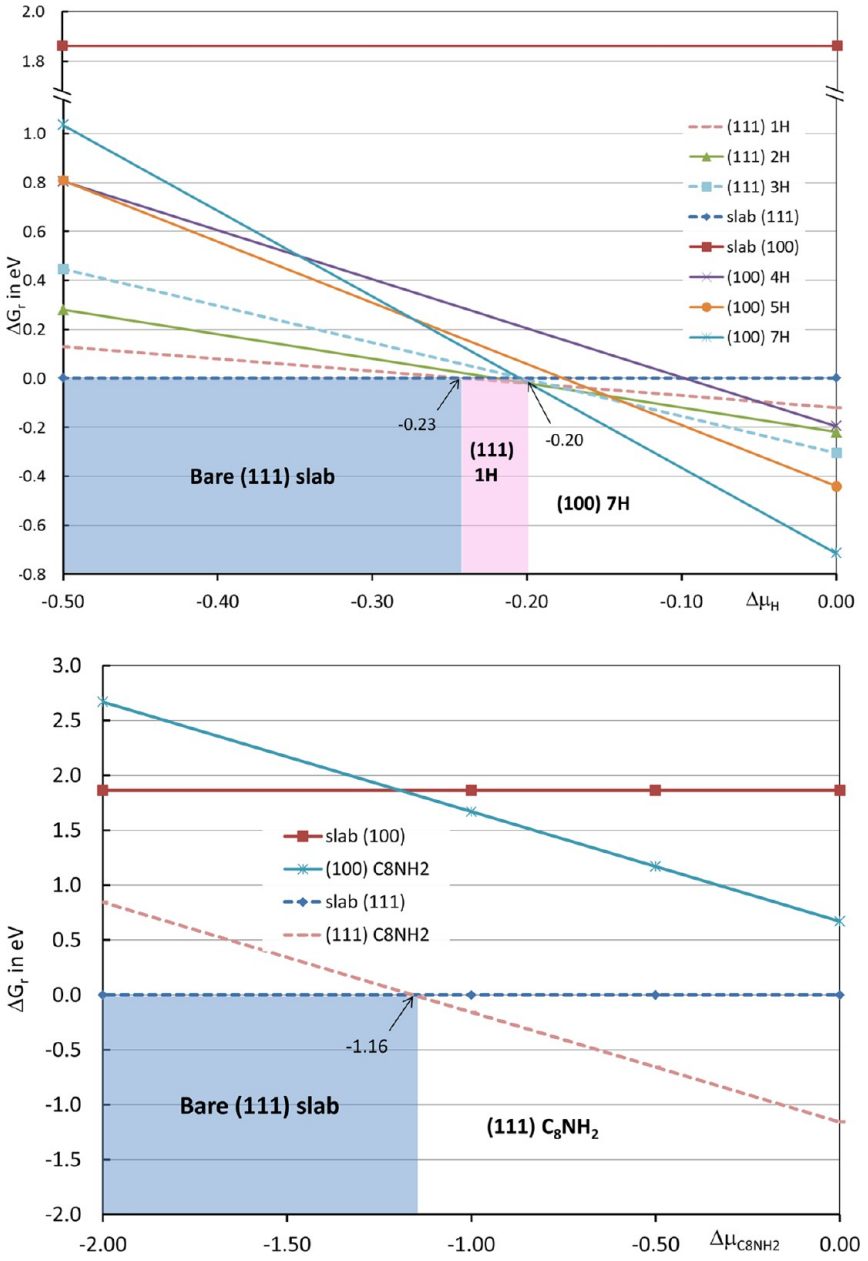

Figure 5. Diagrams of ΔG vs $\Delta\mu$ for the H-covered and C_8NH_2 covered slabs. The most stable system corresponds to the lowest energy line. For the H-covered slabs, the chemical potential represented here is relative to $1/2H_2$ and is denoted as $\Delta\mu_H$, indicating that only $\Delta\mu_H < 0$ are meaningful (above this value H_2 would condensate).

stoichiometric coefficient. This formulation allows a direct comparison of the most stable surfaces for different composition: a straight line with slope −N can be plotted as a function of μ_M for different content in M. For a given chemical potential, the predominant surface will be that of lower energy. This approach is well-suited to our case study, because in the experimental synthesis, the chemical environment is the same for the two terminations (111) and (100). The ΔG diagrams for all the hydrogen-covered calculated slabs are presented in Figure S2. We have represented the most stable hydrogenated slabs for the two terminations taking as reference the most stable (111) slab in Figure 5. It can be observed that for low (very negative) hydrogen chemical potentials, the most stable system is the bare (111) slab. At $\Delta\mu_H$ values between −0.23 eV and −0.20 eV, the 1H-(111) covered slab is the most stable, whereas for higher $\Delta\mu_H$ values, the 7H-(100) slab becomes the most stable system. These data allow us to make the following interpretations: (i) High content of hydrogen is needed to hydrogenate the platinum slabs. The $\Delta\mu_H = -0.23$ eV is indeed a large value compared to metal oxides (−2.21 eV for ZnO, for instance[27]). (ii) The most stable hydrogenated slab corresponds to the (100) termination, and the hydrogenated (111) slabs is stable only in a narrow range of hydrogen chemical potentials (i.e., between −0.23 and −0.20 eV).

The chemical potential of H_2 can be related to the external pressure by means of eq 3

$$\mu = \mu^0 + K_B T \ln(p/p^0) \quad (3)$$

where μ is the chemical potential, μ^0 is the standard chemical potential (tabulated), K_B is the perfect gas constant, T is the temperature, and p/p^0 the pressure/standard pressure. Taking

dx.doi.org/10.1021/jp502174b | J. Phys. Chem. C XXXX, XXX, XXX−XXX

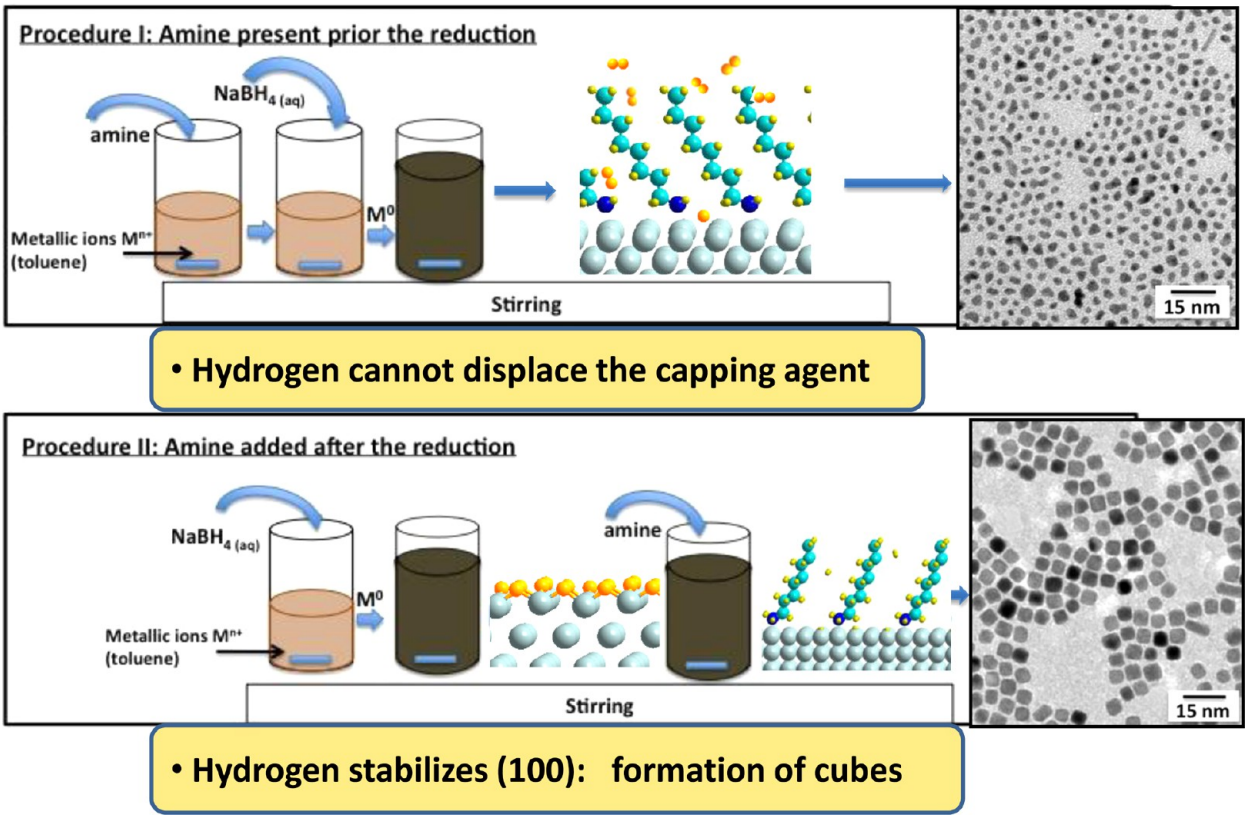

Figure 6. Scheme of the two experimental protocols used in the chemical synthesis. In procedure I, the capping agent is added first, so octylamine stabilizes the (111) termination; in a second step, the reducing agent is added, the hydrogen formed is not able to displace it, and small isotropic particles are formed. In procedure II, the addition of the reducing agent takes place first, and H_2 is formed and preferentially stabilizes the (100) termination. The higher affinity of octylamine for the platinum surfaces displaces the hydrogen, and the cubic shape is preserved.

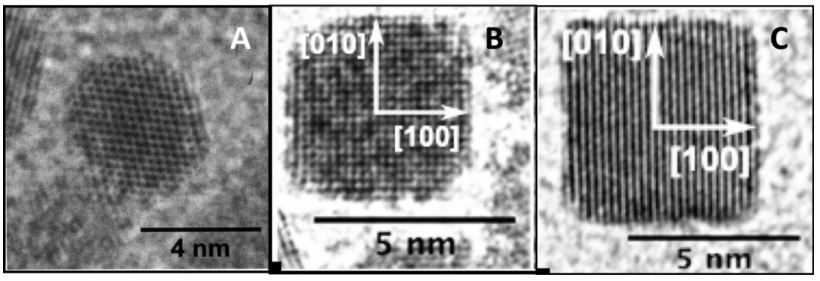

Figure 7. High-resolution TEM images of platinum nanocrystals coated by octylamine and redispersed in toluene. A drop of solution is deposited on a TEM grid. Syntheses are completed following the procedure II, but the capping agent is added (A) 45 min after the reducing agent, (B) 60 min after the reducing agent, and (C) 90 min after the reducing agent.

the value of chemical potential for which the (100) hydrogenated slab starts being dominant $\Delta\mu_H = -0.20$ eV (Figure 5), and at room temperature, the corresponding pressure obtained by eq 3 is 1.18 atm.

DISCUSSION

The results presented above allow us to explain two experimental facts. First, the findings help explain the order of addition of the reactants during the synthesis. In procedure I, the surfactant is added before the reducing agent. The higher affinity of octylamine for the platinum surfaces compared to hydrogen (adsorption energy around −1 eV for C_8NH_2, −0.5 eV for H_2, see Table 1) make the surfaces being covered by C_8NH_2. Because octylamine has no preference for (111) or (100) surfaces, the particles do not show a preferential termination. The particles obtained by this procedure are therefore small and isotropic. In procedure II, the reducing agent is added first, and the in situ generated hydrogen in contact with the metallic particles stabilizes the (100) termination and promotes the formation of cubic shapes. The subsequent addition of octylamine would displace the surface hydrogen due to its higher affinity for platinum, stabilizing the cubic shape. These results are summarized schematically in Figure 6. f6

Second, moderate pressures of hydrogen are needed to obtain the nanocubes, which means high chemical potential of hydrogen. According to the ΔG diagram of Figure 5, at $\Delta\mu_H = -0.20$ eV, the (100) termination responsible for the cubic shape starts being the most stable. Translating the chemical potential into pressure using eq 3 gives a H_2 pressure of 1.18 atm. This pressure is obtained experimentally by using closed vessels. When the capping agent octylamine is added, it displaces hydrogen on the surface and protects the particle. Hence, the

dx.doi.org/10.1021/jp502174b | J. Phys. Chem. C XXXX, XXX, XXX−XXX

nanocrystals grow in the [111] direction, yielding to the cubic shape of the final product.

We can go further and explain the shape control from truncated octahedron to cubic shape, depending on the moment where the capping agent is added, as reported previously.[20] Figure 7 shows HR-TEM picture of nanocrystals obtained by procedure II but waiting 45 min (Figure 7A), 60 min (Figure 7B), and 90 min (Figure 7C) before the addition of the capping agent. In this procedure, the vessel is opened to introduce the passivating agent, thus the hydrogen pressure strongly decreases, and H_2 is released. In fact, if we shorten the time at which the passivating agent is introduced, the particles are no longer cubic but have a much larger truncation. We interpret this result as follows: the hydrogen pressure decreases upon the opening of the vessel and so does the hydrogen chemical potential, inducing a lower stabilization of the (100)-hydrogenated slab compared to (111)-hydrogenated one. This fact promotes the truncation and the formation of the cuboctahedron or truncated octahedron shown in Figure 7. Therefore, the time of exposure to hydrogen partial pressures is a way of controlling the degree of truncation of the nanocubes.

CONCLUSION

The shape control in the chemical synthesis of platinum nanoparticles has been studied by means of periodic DFT calculations and experimental observations. The role of the in situ generated hydrogen and of the surfactant used in the synthesis is evidenced and explained with a theoretical surface slab model. The adsorption energy calculated from DFT allows understanding the preferential interaction of H with (100) terminations, explaining why stable cubes can be obtained when H_2 is present in the medium. Indeed, the external conditions of moderate hydrogen pressure are needed and can be estimated from the DFT calculation to be around 1 atm. An experimental protocol to obtain platinum nanocubes with a controlled degree of truncation has been set up on the basis of the theoretical results.

The above results are an illustration on how standard DFT calculations can be used to rationalize the mechanisms stabilizing nanoparticles on a molecular level. Theory can be used to understand experimental results and may also help orienting the experimentalists in the choice of reactants (selective interaction with given terminations, strength of interaction with the slabs) and experimental conditions (pressure, temperature, order of addition of reactants). Such an approach opens the door to a rational design of experiments beyond the trial−error procedure often followed in chemical synthesis.

ASSOCIATED CONTENT

Supporting Information

Evolution of the adsorption energy per hydrogen with the hydrogen content (Figure S1), ΔG vs μ diagram for H-covered slabs (Figure S2), and dispersion D2 parameters used for the calculations. This material is available free of charge via the Internet at http://pubs.acs.org.

AUTHOR INFORMATION

Corresponding Authors

*E-mail: (M.C.) calatayud@lct.jussieu.fr. Tel.: +33 1 44 27 25 05.
*E-mail: (C.P.) christophe.petit@upmc.fr. Tel.: +33 1 44 27 29 06.

Notes

The authors declare no competing financial interest.

ACKNOWLEDGMENTS

SMART-IP2CT and Erasmus Program is acknowledged for financial support (to N.A.-P.). This work was performed using HPC resources from GENCI- CINES/IDRIS (grants x2011082131, x2012082131, and x2013082131 for 2011−2013, respectively) and the CCRE-DSI of Université P. M. Curie. Boubakar Diawara is warmly acknowledged for providing us with the Modelview visualization program.

REFERENCES

(1) *Complex-Shaped Metal Nanoparticles: Bottom-up Syntheses and Application*Sau, T. K., Rogach, A. L. , Eds.; Wiley-VCH: Weinheim, Germany, 2012.
(2) Petit, C.; Salzemann, C.; Demortière, A. Platinum and Paladium Nanocrystals: Soft Chemistry Approach to Shape Control from Individual Particles to their Self-assembled Superlattices. In *Complex-Shaped Metal Nanoparticles: Bottom-Up Syntheses and Application*, Sau, T. K., Rogach, A. L., Eds. Wiley-VCH: Weinheim, Germany, 2012.
(3) Salzemann, C.; Petit, C. Influence of Hydrogen on the Morphology of Platinum and Palladium Nanocrystals. *Langmuir* **2012**, *28*, 4835−4841.
(4) Chen, M.; Wu, B.; Yang, J.; Zheng, N. Small Adsorbate-Assisted Shape Control of Pd and Pt Nanocrystals. *Adv. Mater.* **2012**, *24*, 862−879.
(5) Bealing, C. R.; Baumgardner, W. J.; Choi, J. J.; Hanrath, T.; Hennig, R. G. Predicting Nanocrystal Shape through Consideration of Surface−Ligand Interactions. *ACS Nano* **2012**, *6*, 2118−2127.
(6) Chiu, C.-Y.; Li, Y.; Ruan, L.; Ye, X.; Murray, C. B.; Huang, Y. Platinum Nanocrystals Selectively Shaped Using Facet-Specific Peptide Sequences. *Nat. Chem.* **2011**, *3*, 393−399.
(7) Petroski, J. M.; Wang, Z. L.; Green, T. C.; El-Sayed, M. A. Kinetically Controlled Growth and Shape Formation Mechanism of Platinum Nanoparticles. *J. Phys. Chem. B* **1998**, *102*, 3316−3320.
(8) Xia, Y.; Xiong, Y.; Lim, B.; Skrabalak, S. E. Shape-Controlled Synthesis of Metal Nanocrystals: Simple Chemistry Meets Complex Physics? *Angew. Chem., Int. Ed.* **2009**, *48*, 60−103.
(9) Scopece, D. SOWOS: an Open-source Program for the Three-Dimensional Wulff Construction. *J. Appl. Crystallogr.* **2003**, *7*, 21−26.
(10) Brust, M.; Walker, M.; Bethell, D.; Schiffrin, D. J.; Whyman, R. Synthesis of Thiol-Derivatised Gold Nanoparticles in a Two-Phase Liquid−Liquid System. *J. Chem. Soc., Chem. Commun.* **1994**, *0*, 801−802.
(11) Petit, C.; Repain, V. Nucleation and Growth of Bimetallic Nanoparticles. In *Nanoalloys: Synthesis, Structure and Properties*; Alloyeau, D., Mottet, C., Ricolleau, C., Eds.; Springer Verlag: New York, 2012; 1−24.
(12) Kresse, G.; Hafner, J. Ab Initio Molecular Dynamics for Liquid Metals. *Phys. Rev. B* **1993**, *47*, 558.
(13) Kresse, G.; Hafner, J. Ab Initio Molecular-Dynamics Simulation of the Liquid-Metal-Amorphous-Semiconductor Transition in Germanium. *Phys. Rev. B* **1994**, *49*, 14251.
(14) Blochl, P. E. Projector Augmented-Wave Method. *Phys. Rev. B* **1994**, *50*, 17953−17979.
(15) Kresse, G.; Joubert, D. From Ultrasoft Pseudopotentials to the Projector Augmented-Wave Method. *Phys. Rev. B* **1999**, *59*, 1758−1775.
(16) Luque, N. B.; Santos, E.; Andres, J.; Tielens, F. Effect of Coverage and Defects on the Adsorption of Propanethiol on Au(111) Surface: A Theoretical Study. *Langmuir* **2011**, *27*, 14514−14521.
(17) Tielens, F.; Costa, D.; Humblot, V.; Pradier, C. M. Characterization Of Omega-Functionalized Undecanethiol Mixed Self-Assembled Monolayers on Au(111): A Combined Polarization Modulation Infrared Reflection-Absorption Spectroscopy/X-Ray Photoelectron Spectroscopy/Periodic Density Functional Theory Study. *J. Phys. Chem. C* **2008**, *112*, 182−190.

(18) Grimme, S. Semiempirical GGA-type Density Functional Constructed with a Long-Range Dispersion Correction. *J. Comput. Chem.* **2006**, *27*, 1787.
(19) Mercurio, G.; McNellis, E. R.; Martin, I.; Hagen, S.; Leyssner, F.; Soubatch, S.; Meyer, J.; Wolf, M.; Tegeder, P.; Tautz, F. S.; Reuter, K. Structure and Energetics of Azobenzene on Ag(111): Benchmarking Semiempirical Dispersion Correction Approaches. *Phys. Rev. Lett.* **2010**, *104*, 036102.
(20) Demortieres, A.; Launois, P.; Goubet, N.; Albouy, P. A.; Petit, C. Shape-Controlled Platinum Nanocubes and Their Assembly into Two-Dimensional and Three-Dimensional Superlattices. *J. Phys. Chem. B* **2008**, *112*, 14583−14592.
(21) Vitos, L.; Ruban, A. V.; Skriver, H. L.; Kollar, J. The Surface Energy of Metals. *Surf. Sci.* **1998**, *411*, 186−202.
(22) Luntz, A. C.; Brown, J. K.; Williams, M. D. Molecular Beam Studies of H_2 and D_2 Dissociative Chemisorption on Pt(111). *J. Chem. Phys.* **1990**, *93*, 5240−5246.
(23) Olsen, R. A.; Kroes, G. J.; Baerends, E. J. Atomic and Molecular Hydrogen Interacting with Pt(111). *J. Chem. Phys.* **1999**, *111*, 11155−11163.
(24) Pijper, E.; Kroes, G. J.; Olsen, R. A.; Baerends, E. J. The Effect of Corrugation on the Quantum Dynamics of Dissociative and Diffractive Scattering of H_2 from Pt(111). *J. Chem. Phys.* **2000**, *113*, 8300−8312.
(25) Ford, D. C.; Xu, Y.; Mavrikakis, M. Atomic and Molecular Adsorption on Pt(111). *Surf. Sci.* **2005**, *587*, 159−174.
(26) Ferrin, P.; Kandoi, S.; Nilekar, A. U.; Mavrikakis, M. Hydrogen Adsorption, Absorption And Diffusion on and in Transition Metal Surfaces: A DFT study. *Surf. Sci.* **2012**, *606*, 679−689.
(27) Meyer, B. First-Principles Study of the Polar O-terminated ZnO Surface in Thermodynamic Equilibrium with Oxygen and Hydrogen. *Phys. Rev. B* **2004**, *69*, 045416.